

Short $\text{N}^+—\text{H}\cdots\text{Ph}$ hydrogen bonds in ammonium tetraphenylborate characterized by neutron diffraction

Thomas Steiner^{a*} and Sax A. Mason^b

^aInstitut für Chemie – Kristallographie, Freie Universität Berlin, Takustrasse 6, D-14195 Berlin, Germany, and ^bInstitut Laue–Langevin, BP 156, 38042 Grenoble CEDEX 9, France

Correspondence e-mail:
steiner@chemie.fu-berlin.de

Received 2 July 1999
Accepted 27 September 1999

The crystal structures of ammonium tetraphenylborate, $\text{NH}_4^+\cdot\text{BPh}_4^-$, are determined by neutron diffraction at 20 and 293 K. At both temperatures, all four N—H vectors of the ammonium ion are time-average-oriented at the midpoints of the phenyl rings of neighboring anions. The N—H \cdots Ph distances, H \cdots M 2.067 and N \cdots M 3.023 Å, are exceptionally short (M = aromatic midpoint). Even at 20 K the ammonium ion performs large amplitude motions which allow the N—H vectors to sample the entire face of the aromatic system.

1. Introduction

Hydrogen bonds with π -bonded moieties acting as the acceptor were discovered by vibrational spectroscopy long ago (Wulf *et al.*, 1936), but they have attracted much attention from structural chemists only recently. Today, structural studies are available of X—H $\cdots\pi$ hydrogen bonds with the X—H donors O—H, N—H, Cl—H, S—H and acidic C—H, and a large number of acceptors such as Ph, $\text{C}\equiv\text{C}$, $\text{C}=\text{C}$, Py, Cp, imidazole, pyrrole, $\text{C}\equiv\text{N}$, SCN^- , and even cyclopropane. As, in principle, these donors and acceptors can form hydrogen bonds in any combination, a great variety of different X—H $\cdots\pi$ bonds occur. Many of these are rather exotic and have been observed in only very few crystal structures, but others occur frequently in certain substance classes. In particular, X—H \cdots Ph hydrogen bonds ('aromatic hydrogen bonds') play an important role in the crystal chemistry of amines and in recognition processes in biology. An overview of the broad field of X—H $\cdots\pi$ interactions has been given by Desiraju & Steiner (1999).

One must distinguish X—H $\cdots\pi$ interactions between uncharged groups and those involving ions. The former normally have energies $\leq 20 \text{ kJ mol}^{-1}$, which is similar to or smaller than energies of conventional O—H \cdots O and N—H \cdots O hydrogen bonds. The interactions of positively charged groups with π -systems are much stronger (Ma & Dougherty, 1997). The dissociation energy of the adduct $\text{NH}_4^+\cdots$ benzene, for example, is 80 kJ mol^{-1} . This energy is mainly due to electrostatic attraction between the positive net charge of NH_4^+ and the π -electron cloud of benzene. Nevertheless, a contact $\text{N}^+—\text{H}\cdots\text{Ph}$ is not exactly the same as a classical cation– π interaction such as $\text{K}^+\cdots\text{Ph}$ (also 80 kJ mol^{-1} in energy), because the directionality characteristics are different. The $\text{N}^+—\text{H}$ vector is not oriented randomly, but tends to point at the aromatic centroid, indicating a significant hydrogen-bond contribution to the total interaction.

Although many relevant crystal structures have been determined by X-ray diffraction, neutron diffraction studies of

$X-H \cdots \pi$ bonding are scarce. Neutron diffraction studies have been reported of an $O-H \cdots C \equiv C$ bond by Allen *et al.* (1996), of an $O-H \cdots Ph$ and a $C \equiv C-H \cdots Ph$ bond by Steiner, Mason & Tamm (1997), of $N-H \cdots Ph$ bonds by Allen *et al.* (1997), and of the $C \equiv C-H \cdots C \equiv C$ interactions in acetylene by McMullan *et al.* (1992). Furthermore, an $N-H \cdots Ph$ bond has been identified in the neutron diffraction crystal structure of coenzyme vitamin B_{12} (Starikov & Steiner, 1998, based on the structure determination by Bouquiere *et al.*, 1993). This paucity of data is not satisfactory and many important types of $X-H \cdots \pi$ bonds have not yet been characterized with neutron techniques at all.

Important model systems to study $X-H \cdots Ph$ interactions with strong ionic contribution (or even ionic dominance) are the tetraphenylborate salts. Knop and co-workers studied salts with various cations containing N^+-H groups and reported statistical data on the many $N^+-H \cdots Ph-B^-$ interactions

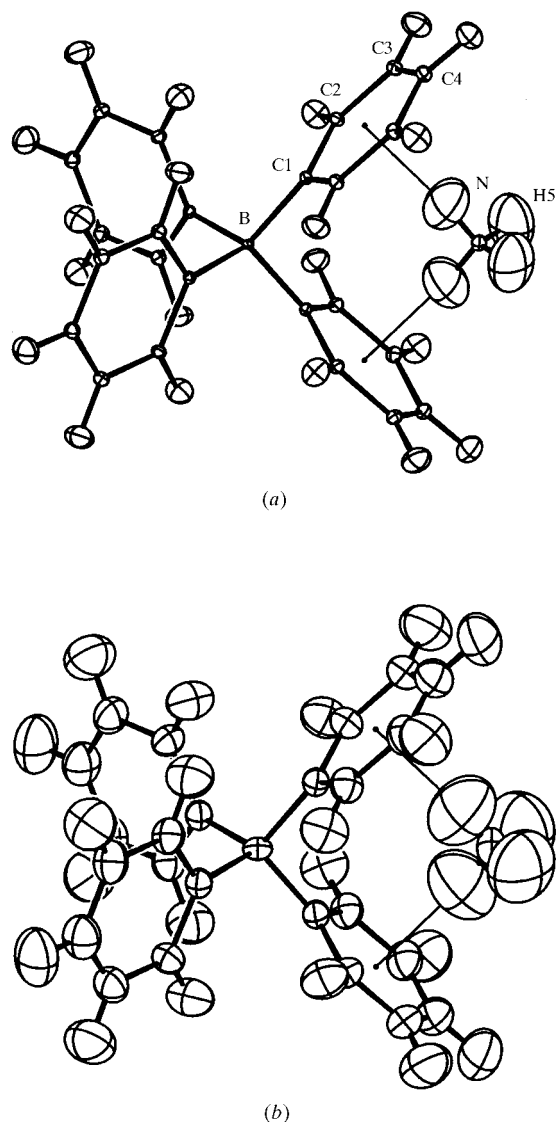


Figure 1
Molecular structure of one formula unit. (a) At 20 K; (b) at 293 K. Displacement ellipsoids are drawn at the 50% probability level.

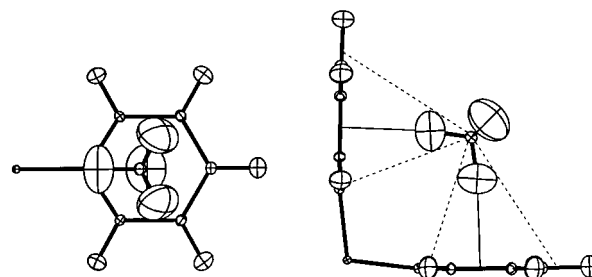


Figure 2
The $N-H \cdots Ph$ interaction in (1) at 20 K shown as projections on and parallel to the aromatic plane. Displacement ellipsoids are drawn at the 50% probability level. The dashed lines in the right figure show the angular region that is sampled by the oscillating $N-H$ vector, based on 50% probability ellipsoids. Note that the individual C atoms are well within this region.

found (Bakshi, Linden *et al.*, 1994). $O-H \cdots Ph-B^-$ bonds formed by water molecules were reported for several hydrated tetraphenylborates (Aubry *et al.*, 1977; Bakshi, Linden *et al.*, 1994; Bakshi, Sereda *et al.*, 1994). $C \equiv C-H \cdots Ph-B^-$ bonds were found in propargylammonium tetraphenylborate and also studied by IR spectroscopy (Steiner, Schreurs *et al.*, 1997). The simplest member of the family, ammonium tetraphenylborate (1), is probably the first substance in which $X-H \cdots \pi$ bonds were observed by X-ray crystallography (Davies & Staveley, 1957). The crystal structure of (1) was re-determined by Westerhaus *et al.* (1980), but even using low-temperature X-ray crystallography, the ammonium protons

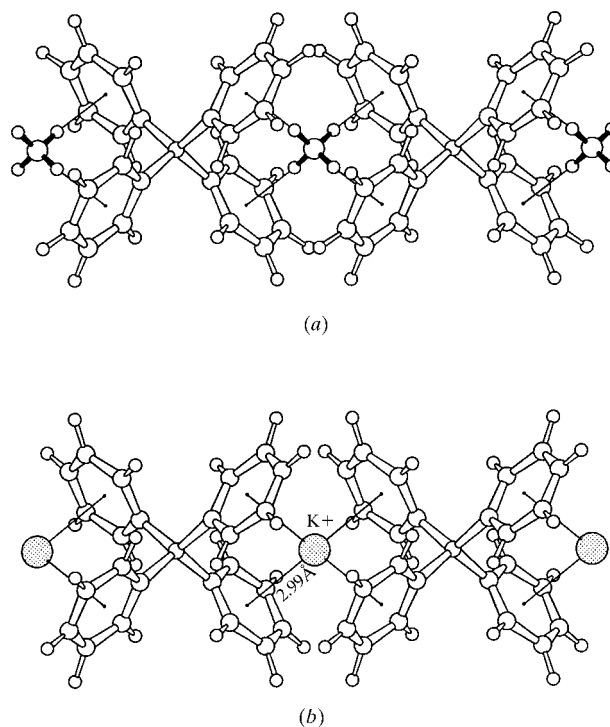
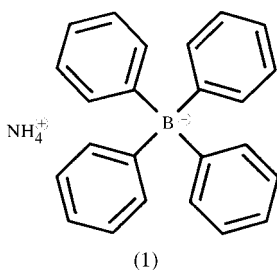


Figure 3
(a) Columns of alternating ammonium and tetraphenylborate ions in (1) (20 K). (b) The isostructural columns in potassium tetraphenylborate (drawn using atomic coordinates from Hoffmann & Weiss, 1974).

could not be located with satisfactory accuracy. Therefore, we have determined the neutron diffraction crystal structure of (1) in order to characterize with high accuracy the geometry of the $\text{N}^+ - \text{H} \cdots \text{Ph} - \text{B}^-$ interaction in this model compound.



2. Experimental

Compound (1) was prepared according to published procedures by mixing aqueous solutions of equimolar amounts of

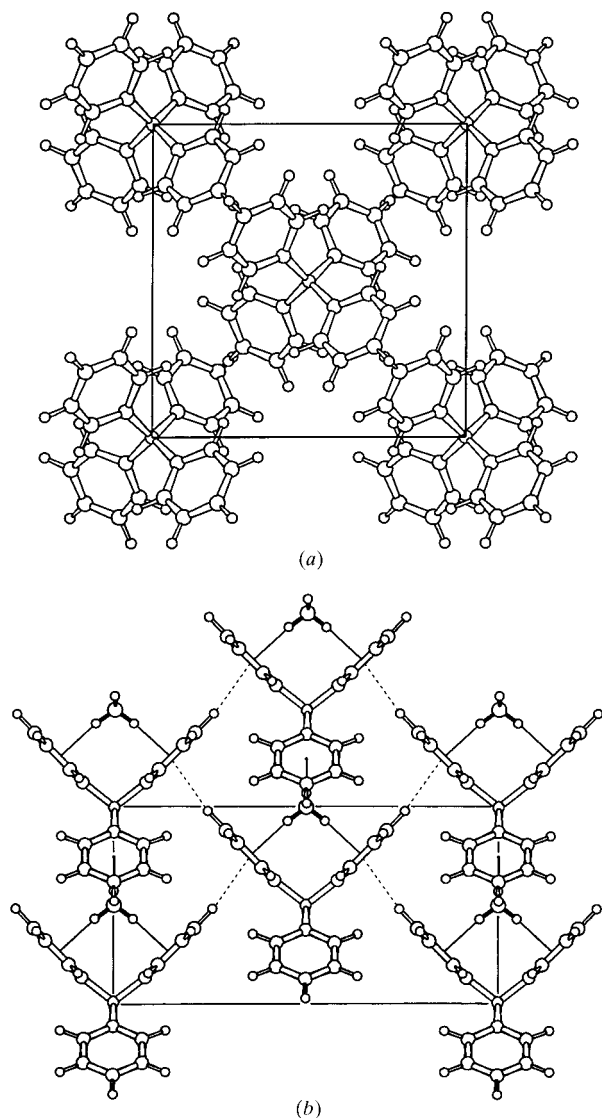


Figure 4
Crystal packing of (1) (20 K). (a) Shown as a projection on the (001) plane, *i.e.* along the column axis; (b) shown as a projection on the (110) plane; $\text{N}-\text{H} \cdots \text{Ph}$ and $\text{C}-\text{H} \cdots \text{Ph}$ contacts are indicated by continuous and dashed lines, respectively.

NaBPh_4 and NH_4Cl (Westerhaus *et al.*, 1980). The white precipitate was repeatedly washed and recrystallized from acetone. To obtain large crystals suitable for neutron diffraction, crystallization experiments were performed with several solvents. The largest crystals were grown by slow evaporation of MeOH solutions.

A crystal of dimensions $0.83 \times 1.00 \times 1.72$ mm, volume 1.4 mm^3 , was glued to an Al pin and sealed in a Displex cryorefrigerator (Archer & Lehmann, 1986) on the D9 hot neutron diffractometer at the high-flux reactor of the Institute Laue-Langevin (ILL). D9 is equipped with an $8 \times 8^\circ$ multiwire (32×32) position-sensitive detector, suitable for accurate measurements of single reflections. The crystal was indexed at room temperature and then cooled to 20 K at -2.5 K min^{-1} . Using a wavelength of $\lambda = 0.8469$ (1) Å, intensities of 1278 reflections were measured at 20 K to a nominal resolution of $\lambda/2\sin \theta_{\text{max}} = 0.60$ Å. Bragg intensities were integrated using the ILL program Racer, with the method of Wilkinson *et al.* (1988). The crystal was then warmed up again at 5.0 K min^{-1} and the intensities of 662 reflections were measured at 293 K. Since time was limited for the experiment, the nominal resolution of the room-temperature data set was only 0.74 Å. Half-wavelength contamination was negligible. Monitoring of a strong reflection during cooling and heating gave no indication of a phase transition. The same three standard reflections were measured every 50 reflections at 20 and 293 K, and showed no significant variation. Finally, the intensities were corrected for attenuation (incoherent scattering and true absorption) by the crystal (calculated $\mu = 2.46 \text{ cm}^{-1}$) with the program *Datap* using a Gaussian integration approximation (Coppens *et al.*, 1965). Full experimental details are given in Table 1.¹

Atomic coordinates of the non-H atoms of the crystal structure determined with X-ray diffraction by Westerhaus *et al.* (1980) were used as the starting model at both temperatures. Neutron scattering lengths were taken from Sears (1992). H-atom positions could immediately be located in difference-Fourier calculations and unconstrained anisotropic refinement (Sheldrick, 1997) proceeded smoothly. Although displacement parameters of the ammonium H atoms are large, there was no indication of split atomic sites (a number of split-atom models were tentatively refined, but gave no convincing and chemically reasonable results). Final fractional atomic coordinates are given in Table 2. The graphics programs used for preparation of the manuscript are *ORTEPII* (Johnson, 1976) and *PLUTON* (Spek, 1995).

3. Results

3.1. General and crystal packing

The anion and cation of (1) are placed on two intersecting mirror planes each, leading to high internal symmetry. Actually, the asymmetric crystal unit (space group $I\bar{4}2m$) contains only 1/8 formula unit of (1). Complete formula units at 20 K

¹ Supplementary data for this paper are available from the IUCr electronic archives (Reference: KA0046). Services for accessing these data are described at the back of the journal.

Table 1
Experimental details.

	Low temperature	Room temperature
Crystal data		
Chemical formula	NH ₄ ⁺ ·C ₂₄ H ₂₀ B ⁻	NH ₄ ⁺ ·C ₂₄ H ₂₀ B ⁻
Chemical formula weight	337.27	337.27
Cell setting	Tetragonal	Tetragonal
Space group	<i>I</i> 42 <i>m</i>	<i>I</i> 42 <i>m</i>
<i>a</i> (Å)	11.1208 (8)	11.2255 (15)
<i>c</i> (Å)	8.0033 (7)	8.0745 (13)
<i>V</i> (Å ³)	989.79 (13)	1017.5 (3)
<i>Z</i>	2	2
<i>Z'</i>	1/8	1/8
<i>D_x</i> (Mg m ⁻³)	1.132	1.101
Radiation type	Neutron	Neutron
Wavelength (Å)	0.8469	0.8469
No. of reflections for cell parameters	354	124
θ range (°)	3.08–44.39	3.07–25.55
μ (mm ⁻¹)	0.246	0.246
Temperature (K)	20	293
Crystal form	Block	Block
Crystal size (mm)	1.72 × 1.00 × 0.83	1.72 × 1.00 × 0.83
Crystal color	Colorless transparent	Colorless transparent
Data collection		
Diffractometer	D9 (at the ILL)	D9 (at the ILL)
Data collection method	Area detector	Area detector
Absorption correction	Gaussian	Gaussian
<i>T_{min}</i>	0.761	0.777
<i>T_{max}</i>	0.826	0.826
No. of measured reflections	1278	662
No. of independent reflections	736	418
No. of observed reflections	639	364
Criterion for observed reflections	<i>I</i> > 2σ(<i>I</i>)	<i>I</i> > 2σ(<i>I</i>)
<i>R_{int}</i>	0.0303	0.0394
θ_{\max} (°)	45.1	34.8
Range of <i>h, k, l</i>	−10 → <i>h</i> → 18 −6 → <i>k</i> → 18 0 → <i>l</i> → 13	−10 → <i>h</i> → 15 −6 → <i>k</i> → 15 0 → <i>l</i> → 10
No. of standard reflections	3	3
Frequency of standard reflections	Every 50 reflections	Every 50 reflections
Intensity decay	Not significant	Not significant
Refinement		
Refinement on	<i>F</i> ²	<i>F</i> ²
<i>R</i> [<i>F</i> ² > 2σ(<i>F</i> ²)]	0.038	0.069
<i>wR</i> (<i>F</i> ²)	0.066	0.116
<i>S</i>	1.098	1.225
No. of reflections used in refinement	736	418
No. of parameters used	65	65
H-atom treatment	All parameters refined	All parameters refined
Weighting scheme	$w = 1/[\sigma^2(F_o^2) + 5.0563P]$, where $P = (F_o^2 + 2F_c^2)/3$	$w = 1/[\sigma^2(F_o^2) + 7.8251P]$, where $P = (F_o^2 + 2F_c^2)/3$
(Δ/σ) _{max}	< 0.001	< 0.001
$\Delta\rho_{\max}$ (e Å ⁻³)	1.38	0.64
$\Delta\rho_{\min}$ (e Å ⁻³)	−1.14	−0.57
Extinction method	None	None
Source of atomic scattering factors	<i>International Tables for Crystallography</i> (1992, Vol. C, Tables 4.2.6.8 and 6.1.1.4)	<i>International Tables for Crystallography</i> (1992, Vol. C, Tables 4.2.6.8 and 6.1.1.4)
Computer programs		
Structure refinement	<i>SHELXL97</i> (Sheldrick, 1997)	<i>SHELXL97</i> (Sheldrick, 1997)

and room temperature are shown in Fig. 1. The structure is virtually identical at both temperatures, apart from the much larger displacement parameters at room temperature. Relevant geometrical data are given in Table 3 for both tempera-

tures. Upon cooling, the unit cell shrinks almost isotropically (Table 4), so that there are almost no shifts of the molecules with respect to each other and no substantial changes in the intermolecular interactions. This justifies concentrating on the much more accurate 20 K structure in the following.

In (1) each of the N⁺—H vectors is oriented almost exactly toward the midpoint of the phenyl ring of an anion, Fig. 2. The distances to the aromatic centroid *M* are 2.067 Å for the H atom and 3.023 Å for the N atom (these and all the following values at 20 K). This interaction will be discussed in greater detail below. The conformation of the anion is determined by optimization of the N⁺—H···Ph interactions. The covalent angles around the B atom are markedly distorted from tetrahedral geometry, with one of the two symmetry-independent C—B—C angles reduced to 103.64 (10)° and the other one opened up to 112.46 (5)°. The phenyl groups are oriented in such a way that there are two pairs of almost perpendicular aromatic rings [interplanar angle 90.82 (3)°]. This is accompanied by bending of the B—C1 vector out of the aromatic plane [B—C1···C4 angle 172.76 (8)°]. This geometry allows the cation to be chelated by two phenyl rings of the anion, with close to optimal N⁺—H···Ph interactions. Similarly pronounced distortions of BPh₄⁻ anions were reported by Bakshi, Linden *et al.* (1994). The distortions can be explained by the high energy of the cation–π interaction involved.

The ammonium ion has close to tetrahedral conformation, the two symmetry-independent H—N—H angles being 107.2 (13)

and 110.6 (7)°. The N—H bond length of 0.960 (7) Å (at 20 K) is reduced by 0.069 Å compared with the gas-phase value of 1.029 Å (Crofton & Oka, 1987). This apparent shortening can be explained as a typical thermal vibration artefact associated

Table 2

Fractional atomic coordinates and equivalent isotropic displacement parameters (\AA^2).

$$U_{\text{eq}} = (1/3)\sum_i \sum_j U^{ij} a^i a^j \mathbf{a}_i \cdot \mathbf{a}_j.$$

	<i>x</i>	<i>y</i>	<i>z</i>	<i>U</i> _{eq}
(1) at 20 K				
B	0	0	0	0.0034 (5)
N	0	0	1/2	0.0080 (3)
C1	0.08200 (9)	0.08200 (9)	0.12672 (18)	0.0048 (2)
C2	0.04000 (9)	0.19147 (9)	0.19306 (14)	0.00640 (16)
C3	0.10202 (9)	0.25438 (9)	0.31756 (14)	0.00746 (17)
C4	0.20961 (10)	0.20961 (10)	0.38113 (19)	0.0079 (2)
H2	-0.0455 (2)	0.2280 (2)	0.1484 (3)	0.0209 (5)
H3	0.0649 (3)	0.3379 (2)	0.3653 (4)	0.0239 (5)
H4	0.2569 (3)	0.2569 (3)	0.4807 (5)	0.0228 (7)
H5	0.0491 (5)	0.0491 (5)	0.4288 (12)	0.092 (4)
(1) at 293 K				
B	0	0	0	0.0211 (17)
N	0	0	1/2	0.0421 (16)
C1	0.0811 (2)	0.0811 (2)	0.1255 (5)	0.0255 (8)
C2	0.0399 (3)	0.1897 (3)	0.1917 (4)	0.0359 (7)
C3	0.1009 (4)	0.2518 (3)	0.3156 (5)	0.0459 (9)
C4	0.2077 (3)	0.2077 (3)	0.3782 (8)	0.0535 (14)
H2	-0.0444 (8)	0.2267 (7)	0.1447 (12)	0.063 (2)
H3	0.0670 (10)	0.3354 (9)	0.3603 (13)	0.081 (3)
H4	0.2557 (11)	0.2557 (11)	0.4756 (17)	0.091 (5)
H5	0.0456 (17)	0.0456 (17)	0.437 (3)	0.162 (12)

with the large mean displacement of the ammonium H atoms from their mean positions even at 20 K (see Fig. 1).

In the crystal, cations and anions are arranged in columns along the tetragonal *c* axis. In these columns the cations form $\text{N}^+ - \text{H} \cdots \text{Ph}$ interactions with four phenyl rings of two neighboring anions, Fig. 3(a). The phenyl rings form a kind of aromatic capsule, in which the ammonium ion is neatly embedded. The columns are arranged in the unit cell as shown in Fig. 4. Between the columns, there are short lateral contacts in a diagonal plane of the unit cell, Fig. 4(b). In these contacts,

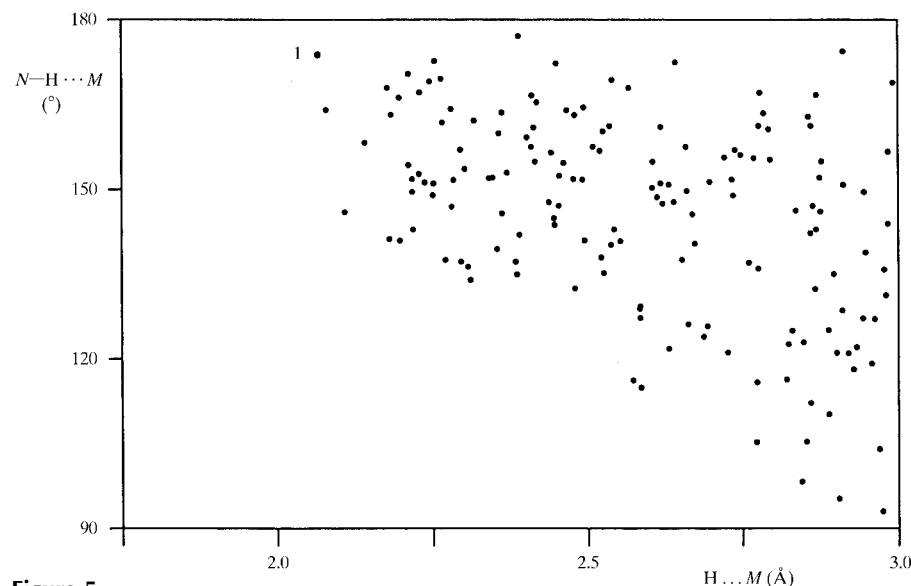


Figure 5

Geometry of $\text{N}-\text{H} \cdots \text{M}$ interactions in 79 tetraphenylborate salts. *M* denotes the aromatic centroid. Multifurcated interactions are fully considered. The data point from (1) at 20 K is marked.

Table 3

Geometrical data.

	<i>T</i> = 20 K	<i>T</i> = 293 K
Covalent geometry, anion		
B—C1 (Å)	1.6406 (14)	1.638 (4)
C—C, mean (Å)	1.3998 (13)	1.400 (4)
C—H, mean (Å)	1.090 (3)	1.090 (9)
C1—B—C1' (°)	103.64 (10)	103.6 (3)
C1—B—C1'' (°)	112.46 (5)	112.49 (14)
B—C1...C4 (°)	172.76 (8)	172.8 (2)
Covalent geometry, cation		
N—H5 (Å)	0.960 (7)	0.89 (2)
H5—N—H5' (°)	107.2 (13)	110 (4)
H5—N—H5'' (°)	110.6 (7)	109 (2)
$\text{N}^+ - \text{H} \cdots \text{Ph}$ interaction		
H5...C range (Å)	2.472 (9)–2.553 (8)	2.56 (2)–2.62 (2)
N...C range (Å)	3.254 (2)–3.431 (2)	3.287 (4)–3.441 (5)
N—H5...C range (°)	138.5 (9)–152.2 (9)	138 (3)–155 (3)
H...M (Å)	2.067	2.17
N...M (Å)	3.023	3.04
N—H...M (°)	173.8	172
ω_{H5} (°)	1.9	1.0
ω_{N} (°)	3.9	3.4
N...B (Å)	4.0017 (4)	4.0372 (6)
$\text{C4}-\text{H} \cdots \text{Ph}$ interaction		
H4...C range (Å)	2.791 (4)–3.248 (4)	2.86 (2)–3.30 (2)
C4...C range (Å)	3.822 (2)–4.199 (1)	3.902 (6)–4.255 (3)
C4—H...C range (°)	156.3 (3)–157.8 (3)	146 (1)–159 (1)
H4...M (Å)	2.670	2.74
C4...M (Å)	3.751	3.82
C4—H...M (°)	172.0	171
ω_{H4} (°)	8.1	7.5
ω_{C4} (°)	10.4	10.0

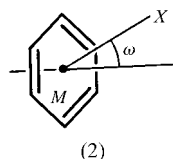
phenyl rings of neighboring anions form herringbone-type $\text{Ph} \cdots \text{Ph}$ interactions, with quite a short distance of 2.67 Å from the atom H4 to the aromatic center (Table 3). The $\text{B}^- \cdots \text{B}^-$ distance of the contacting ions is 8.823 Å. Interestingly, these are inter-anion contacts that do not seem to be

mediated by direct interactions with the cations. To some degree, this is reminiscent of the inter-cation $\text{Ph} \cdots \text{Ph}$ interactions that occur very frequently between tetraphenylphosphonium ions (Dance & Scudder, 1996).

It is of interest that the K^+ and Rb^+ tetraphenylborates are isostructural with (1) (K^+ salt: Hoffmann & Weiss, 1974; Rb^+ salt: Ozol *et al.*, 1962). This is illustrated for the K^+ salt in Fig. 3(b). The cation...*M*(Ph) distances are 2.99 Å for K^+ and 3.17 Å for Rb^+ , and the individual cation...C distances are in the range 3.19–3.40 Å for K^+ and 3.40–3.47 Å for Rb^+ . These short contacts represent interactions of the pure cation- π type. One should note that the $\text{NH}_4^+ \cdots \text{Ph}$ separation in (1) (3.02 Å) is almost identical to the $\text{K}^+ \cdots \text{Ph}$ distance in K^+BPh_4^- .

3.2. The $N^+—H \cdots Ph$ interaction

The geometry of the $N^+—H \cdots Ph$ interaction is given in detail in Table 3. The distance of the H atom to the aromatic centroid M , 2.067 Å, is much shorter than the distance to any of the individual C atoms (distance range 2.47–2.55 Å). On normalizing the N—H bond to the gas-phase bond length, the $H \cdots M$ distance becomes 2.00 Å and the range of $H \cdots C$ distances becomes 2.41–2.49 Å. The angles ω as defined in (2) are close to 0° , showing that the interaction is close to centered. As is seen in the left part of Fig. 2, the ammonium H atom is placed almost exactly over the aromatic centroid.



The ammonium H atom has by far the largest displacement parameters in the crystal structure. Even at 20 K, U_{eq} of H5 is 0.092 (4) Å², to be compared with the mean U_{eq} of 0.023 for the other H atoms. Positional disorder involving discrete alternative sites, however, was not apparent in the refinement. The shape of the displacement ellipsoid suggests the occurrence of large amplitude librations of the cation around the central N atom. This has consequences for the fundamental problem: which part of the phenyl ring has to be considered as the acceptor of the hydrogen bond. It is only on the time-average that the N—H vector points towards the aromatic midpoint. When taking the 50% probability ellipsoids in Fig. 2 as a reference, it is seen that during its motion, the N—H vector actually samples the entire face of the aromatic ring, including the individual C atoms (dashed lines in Fig. 2, right). It would be desirable to obtain a better picture of the true, non-Gaussian probability density function (p.d.f.) of H, but this is not feasible with normal refinement methods which are based on fitting p.d.f.s by three-dimensional Gaussians.

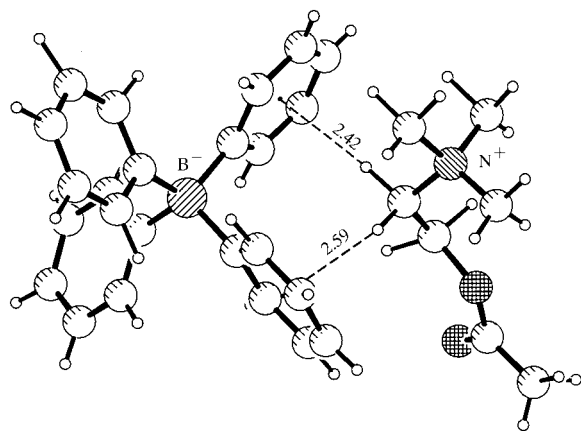


Figure 6
C—H \cdots Ph contacts in acetylcholine tetraphenylborate (drawn using atomic coordinates from Datta *et al.*, 1980). For normalized H-atom positions, the two C—H \cdots Ph contacts have geometries of $H \cdots M$ 2.42, $C \cdots M$ 3.35 Å, $C—H \cdots M$ 143°, and $H' \cdots M'$ 2.59, $C \cdots M'$ 3.67 Å, $C—H' \cdots M'$ 171°, respectively. $C \cdots B$ 4.55, $N^+ \cdots B$ 5.65 Å.

Table 4

Reduction of the unit cell upon cooling to 20 K.

δ = relative difference of values at room temperature and 20 K, $\delta = 100(x_{20K} - x_{RT})/x_{RT}$.

	δ (%)
a	−0.94 (2)
c	−0.88 (2)
V	−2.72 (3)

Table 5

Geometry of N—H \cdots Ph and O—H \cdots Ph interactions in tetraphenylborates (CSD data for normalized H-atom positions).

	N ⁺ —H \cdots Ph—B [−]	O—H \cdots Ph—B [−]
No. of structures	79	11
No. of contacts	165	22
Mean H \cdots M (Å)	2.59 (2)	2.48 (4)
Mean X \cdots M (Å)	3.44 (2)	3.34 (3)
Mean X—H \cdots M (°)	140 (3)	150 (4)
Shortest H \cdots M (Å)	2.07†	2.22
Shortest X \cdots M (Å)	3.02	3.12

† Experimental value in (1) at 20 K; $H \cdots M$ becomes 2.00 Å after normalization of the H-atom position.

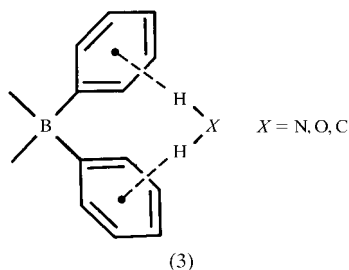
One might also expect that the ammonium ion performs rotational jumps at certain rates and probably these rates are high, but such a phenomenon cannot be observed with diffraction techniques.

3.3. Statistical data and hydrogen-bond pattern

In the tabulations of Bakshi, Linden *et al.* (1994), there is no $N^+—H \cdots Ph$ contact in a BPh_4 salt that is as short as the one in (1). As many BPh_4 crystal structures have been published since then, a new database survey was performed for this type of interaction [Cambridge Structural Database, update 5.16 with 190 307 entries; Allen & Kennard, 1993; ordered BPh_4 salts with $R < 0.08$, combined with (1) at 20 K and the structure from Steiner, Schreurs *et al.*, 1997, which is not yet in the CSD, normalized H-atom positions]. For the $N^+—H \cdots Ph—B^-$ contacts in 79 BPh_4 salts, the scatterplot of N—H \cdots M angles against $H \cdots M$ distances is shown in Fig. 5. For the many multifurcated N—H \cdots Ph contacts that occur in these compounds (*i. e.* interactions of one N—H group with more than one phenyl group, Bakshi, Linden *et al.*, 1994), all components with $H \cdots M < 3.0$ Å are considered. The plot shows the typical directionality characteristics of a hydrogen-bond interaction. At short distances, relatively linear angles are preferred, whereas with increasing distance this preference softens. The data point from (1) (uncorrected for thermal vibrations) is marked in Fig. 5 and represents the shortest, and one of the most linear N—H \cdots Ph interactions in tetraphenylborates. In Table 5, some numerical values are listed for the data in Fig. 5 and some related data for O—H \cdots Ph—B[−] interactions are given for comparison.

Finally, we wish to point out again the chelated motif of $N^+—H \cdots Ph$ interactions in (1) (Figs. 1–3). This motif occurs regularly in tetraphenylborate salts, if the cation is in principle able to form it. For ammonium cations, the requirement is the

presence of at least two $N^+ - H$ donors (that is NH_4^+ , $R - NH_3^+$ and $R_2NH_2^+$ with $R \neq H$; for examples, see Bakshi, Linden *et al.*, 1994; Steiner, Schreurs *et al.*, 1997). It is of general interest that this motif also occurs frequently with other bidentate donors, XH_2 (III). In particular, it has been reported several times with water molecules (Aubry *et al.*, 1977; Bakshi, Linden *et al.*, 1994). The motif can also be formed with $X = C$, for which it has not been explicitly discussed as yet. As a typical example, the structure of acetylcholine tetraphenylborate (Datta *et al.*, 1980) is shown in Fig. 6. Note that the shorter of the two $H \cdots M$ distances is only 2.42 Å; further geometrical data are given in the figure legend. The frequent occurrence of this interaction pattern with chemically diverse cations and even neutral XH_2 groups suggests that it is a major organization principle in tetraphenylborate salts. This fully justifies classification as a supramolecular synthon (Desiraju, 1995). In such a case, one may also wish to apply the graph-set formalism (Etter, 1990; Bernstein *et al.*, 1995) to characterize the hydrogen-bond pattern. If this formalism is applied to π -acceptors, which are always formed by groups of atoms, there is an obvious problem when counting the atoms constituting a motif. The problem can be overcome if the π -acceptor is considered as an entity and counted as a single quasi-atom (suggested for $C \equiv C$ acceptors by Subramanian *et al.*, 1996). Then, the pattern shown in (3) is denoted as a ring of six 'atoms' that contains two donors and two acceptors, $R_2^2(6)$.



TS thanks Professor Wolfram Saenger for the opportunity to carry out part of this study in his laboratory.

References

- Allen, F. H., Howard, J. A. K., Hoy, V. J., Desiraju, G. R., Reddy, D. S. & Wilson, C. C. (1996). *J. Am. Chem. Soc.* **118**, 4081–4084.
- Allen, F. H., Hoy, V. J., Howard, J. A. K., Thalladi, V. R., Desiraju, G. R., Wilson, C. C. & McIntyre, G. J. (1997). *J. Am. Chem. Soc.* **119**, 3477–3480.
- Allen, F. H. & Kennard, O. (1993). *Chem. Des. Autom. News*, **8**, 1.
- Archer, J. & Lehmann, M. S. (1986). *J. Appl. Cryst.* **19**, 456–458.
- Aubry, A., Protas, J., Moreno-Gonzales, E. & Marraud, M. (1977). *Acta Cryst.* **B33**, 2572–2578.
- Bakshi, P. K., Linden, A., Vincent, B. R., Roe, S. P., Adhikesavalu, D., Cameron, T. S. & Knop, O. (1994). *Can. J. Chem.* **72**, 1273–1293.
- Bakshi, P. K., Sereda, S. V., Knop, O. & Falk, M. (1994). *Can. J. Chem.* **72**, 2144–2152.
- Bernstein, J., Davis, R. E., Shimoni, L. & Chang, N.-L. (1995). *Angew. Chem. Int. Ed. Engl.* **34**, 1555–1573.
- Bouquiere, J. P., Finney, J. L., Lehmann, M. S., Lindley, P. F. & Savage, H. F. J. (1993). *Acta Cryst.* **B49**, 79–89.
- Coppens, P., Leiserowitz, L. & Rabinovich, D. (1965). *Acta Cryst.* **18**, 1035–1038.
- Crofton, M. W. & Oka, T. (1987). *J. Chem. Phys.* **86**, 5983–5988.
- Dance, I. & Scudder, M. (1996). *Chem. Eur. J.* **2**, 481–486.
- Datta, N., Mondal, P. & Pauling, P. (1980). *Acta Cryst.* **B36**, 906–909.
- Davies, T. & Staveley, L. A. K. (1957). *Trans. Faraday Soc.* **53**, 19–30.
- Desiraju, G. R. (1995). *Angew. Chem. Int. Ed. Engl.* **34**, 2311–2327.
- Desiraju, G. R. & Steiner, T. (1999). *The Weak Hydrogen Bond in Structural Chemistry and Biology*. Oxford University Press.
- Etter, M. C. (1990). *Acc. Chem. Res.* **23**, 120–126.
- Hoffmann, K. & Weiss, E. (1974). *J. Organomet. Chem.* **67**, 221–228.
- Johnson, C. K. (1976). *ORTEP II*. Report ORNL-5138. Oak Ridge National Laboratory, Tennessee, USA.
- Ma, J. C. & Dougherty, D. A. (1997). *Chem. Rev.* **97**, 1303–1324.
- McMullan, R. K., Kvik, A. & Popelier, P. (1992). *Acta Cryst.* **B48**, 726–731.
- Ozol, Y., Vimba, S. & Ievins, A. (1962). *Kristallografija*, **7**, 362.
- Sears, V. F. (1992). *Neutron News*, **3**, 26–37.
- Sheldrick, G. M. (1997). *SHELXL97*. University of Göttingen, Germany.
- Spek, A. L. (1995). *PLUTON*. University of Utrecht, The Netherlands.
- Starikov, E. B. & Steiner, T. (1998). *Acta Cryst.* **B54**, 94–96.
- Steiner, T., Mason, S. A. & Tamm, M. (1997). *Acta Cryst.* **B53**, 843–848.
- Steiner, T., Schreurs, A. M. M., Kanters, J. A., Kroon, J., van der Maas, J. & Lutz, B. (1997). *J. Mol. Struct.* **436/437**, 181–187.
- Subramanian, K., Lakshmi, S., Rajagopalan, K., Koellner, G. & Steiner, T. (1996). *J. Mol. Struct.* **384**, 121–126.
- Westerhaus, W. J., Knop, O. & Falk, M. (1980). *Can. J. Chem.* **58**, 1355–1364.
- Wilkinson, C., Khamis, H. W., Stansfield, R. F. D. & McIntyre, G. J. (1988). *J. Appl. Cryst.* **21**, 471–478.
- Wulf, O. R., Liddel, U. & Hendricks, S. B. (1936). *J. Am. Chem. Soc.* **58**, 2287–2293.